THE REDUCED-INTERFERENCE LOCAL WIGNER-VILLE DISTRIBUTION

Harald Oehlmann *David Brie*

Centre de Recherche en Automatique de Nancy, CNRS URA 821
Université Henri Poincaré, Nancy 1, B.P. 239, 54506 Vandœuvre Cedex (France)
Ph.: (33) 3 83 91 20 69 — Fax: (33) 3 83 91 20 30 — E-Mails: oehlmann@cran.u-nancy.fr, brie@cran.u-nancy.fr

ABSTRACT

The Local Wigner-Ville Distribution (LWVD) extends the Cohen's class time-frequency distributions (TFD) by the definition of a kernel for each time-frequency point(local kernel). The subject of the paper is the determination of these local kernels for interference reduction. Starting from the simple idea of the local limitation of the Wigner-Ville TFD integral bounds, a method is presented to estimate these limits and to obtain a reduced interference TFD. The effectiveness for interference reduction of this LWVD, specially when compared to global-kernel methods, is shown using example signals.

1. INTRODUCTION

Most time-frequency distributions (TFD) use a smoothing kernel to reduce cross-components of the Wigner-Ville Distribution (WVD). The choice of the kernel greatly affects the appearence (and quality) of the TFD. In this framework, a major contribution was given by the work of Baraniuk-Jones [1] who showed that, firstly, the optimal kernel for interference reduction depends on the signal being analised. Secondly, they formulated the problem of optimal kernel design as an optimization problem. However, the use of any fixed (global) kernel limits the class of signals for which the resulting TFD performs well. Some attempts have been made to overcome this limitation by the use of a local kernel in the sense that the kernel depends on time [2, 3]. The work presented in this paper extends this approach by defining a kernel depending explicitly on the time-frequency point considered.

To begin, we may consider the Smoothed Pseudo WVD [4], defined by:

$$\begin{aligned}\mathsf{SPWV}(t,\omega) &= \Phi(t,\omega) \star \mathsf{WV}(t,\omega) \qquad (1)\\ &= \mathcal{F}^{\,2\mathrm{D}}\left\{\phi(\theta,\tau)\cdot A(\theta,\tau)\right\}\end{aligned}$$

where $\mathsf{WV}(t,\omega)$ is the WVD, $A(\theta,\tau)$ is the ambiguity function and $\Phi(t,\omega)$ ($\phi(\theta,\tau)$) is a separable smoothing filter:

$$\Phi(t,\omega) = \Phi^T(\omega)\cdot\Phi^F(t) \quad \phi(\theta,\tau) = \phi^T(\tau)\cdot\phi^F(\theta)$$

The superscript T (resp. F) denotes that the filter is intended to reduce time (resp. frequency) interferences. If we restrict ourselves to rectangular functions:

$$\phi^T(\tau) = \mathrm{rect}_{\tau_{\max}}(\tau) \quad \phi^F(\theta) = \mathrm{rect}_{\theta_{\max}}(\theta) \qquad (2)$$

the effects of the smoothing filters may be interpreted as a limitation of the WVD integral to the bounds $]-\tau_{\max};\tau_{\max}[$:

$$\begin{aligned}\mathsf{SPWV}^T(t,\omega) &= \int_{-\tau_{\max}}^{\tau_{\max}} s^*\left(t-\frac{\tau}{2}\right) s\left(t+\frac{\tau}{2}\right) e^{-j\omega\tau}\,d\tau \qquad (3)\\ \mathsf{SPWV}^F(t,\omega) &= \int_{-\theta_{\max}}^{\theta_{\max}} S\left(\omega-\frac{\theta}{2}\right) S^*\left(\omega+\frac{\theta}{2}\right) e^{-jt\theta}\,d\theta\end{aligned}$$

and the resulting Smoothed Pseudo WVD may be seen as a combination of these two TFDs.

The approach of the Local WVD (LWVD) is to replace the fixed limit $\tau_{\max}$ (resp. $\theta_{\max}$) by a limit $\tau_{\max}(t,\omega)$ (resp. $\theta_{\max}(t,\omega)$) which explicitly depends on the time-frequency point considered. The two TFD are then combined into a reduced interference TFD.

The organisation of this paper is as follows: in section 2. we define the time-product and frequency-product functions. Their study enables us to prove the existence and to evaluate the limits $\tau_{\max}(t,\omega)$ and $\theta_{\max}(t,\omega)$ which are optimal for interference reduction. Moreover, these functions have separation capacities of autoterms and interferences. On the basis of these results, we present in section 3. a scheme to estimate these limits. In section 4., we introduce a new formalism for the local smoothing of the WVD which enables us to interpret the LWVD in terms of a kernel depending explicitly on the time-frequency point considered. In section 5. each step of the method is illustrated by means of an example signal. In addition, a more complicated signal is used to show the good interference reduction capacities of the LWVD. Conclusions and perspectives are given in section 6..

2. THE TIME-PRODUCT AND FREQUENCY-PRODUCT FUNCTIONS

2.1. Definitions

The WVD is defined by:

$$\mathsf{WV}(t,\omega) = \frac{1}{2\pi}\int s^*\left(t-\frac{\tau}{2}\right) s\left(t+\frac{\tau}{2}\right) e^{-j\omega\tau} d\tau$$

and it may be decomposed into the sum of two integrals on the positive real axis:

$$\begin{aligned}\mathsf{WV}(t,\omega) = &\frac{1}{2\pi}\int_{\tau\in[0;\infty[} s^*\left(t-\frac{\tau}{2}\right) s\left(t+\frac{\tau}{2}\right) e^{-j\omega\tau} d\tau \,+\\ &+\frac{1}{2\pi}\int_{\tau\in]0;\infty[} s^*\left(t+\frac{\tau}{2}\right) s\left(t-\frac{\tau}{2}\right) e^{j\omega\tau} d\tau\end{aligned}$$

which, due to the relationship $z + z^* = 2\,\mathcal{R}\{z\}$ may be written as:

$$\mathsf{WV}(t,\omega) = \frac{1}{\pi}\int_0^\infty \mathrm{o}(\tau)\,\mathcal{R}\left\{s^*\left(t-\frac{\tau}{2}\right) s\left(t+\frac{\tau}{2}\right) e^{-j\omega\tau}\right\} d\tau$$

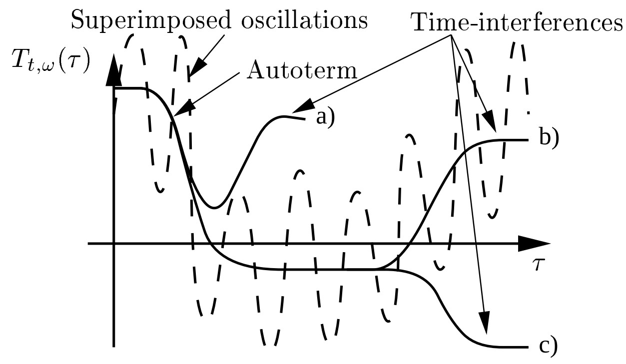

Figure 1. Geometry of the time-product function.

with:

$$\mathrm{o}(\tau) = \begin{cases} 1/2 & \tau = 0 \\ 1 & \tau \neq 0. \end{cases}$$

The time-product function is then defined as the argument of the integral:

$$T_{t,\omega}(\tau) = \mathrm{o}(\tau)\,\Re\left\{ s\left(t+\frac{\tau}{2}\right) s^*\left(t-\frac{\tau}{2}\right) e^{-j\omega\tau} \right\}.$$

The WVD may also be expressed in a dual form involving the Fourier-transform of the signal $S(\omega) = \mathcal{F}\left\{s(t)\right\}$:

$$\mathsf{WV}(t,\omega) = \frac{1}{2\pi}\int_{-\infty}^{\infty} S\left(\omega-\frac{\theta}{2}\right) S^*\left(\omega+\frac{\theta}{2}\right) e^{-jt\theta} d\theta.$$

Making a similar decomposition of the integral we define the frequency-product function as:

$$F_{t,\omega}(\theta) = \mathrm{o}(\theta)\,\Re\left\{ S\left(\omega-\frac{\theta}{2}\right) S^*\left(\omega+\frac{\theta}{2}\right) e^{-jt\theta} \right\}.$$

2.2. Optimal Limits and Properties of the Product Functions

Due to space limitations, we will only give the essential results of the study [5]. For time-separable signals:

$$s(t) = s_1(t) + s_2(t)$$
$$s_1(t) = 0 \quad \text{if } t \notin T_1 =]-\infty; t_1]$$
$$s_2(t) = 0 \quad \text{if } t \notin T_2 = [t_2; \infty[$$

the optimal limits only depend on time and are given by:

$$\tau_{\max}(t) = \begin{cases} -2(t-t_2) & t < \frac{t_1+t_2}{2} \\ 2(t-t_1) & t \geq \frac{t_1+t_2}{2} \end{cases} \qquad \theta_{\max} = \infty. \tag{4}$$

Using time-frequency duality, the optimal limits for frequency-separable signals depend only on frequency and may be expressed in a similar way as equation (4).

The case of non-separable signals is discussed using two example signals, one separable in the time-frequency plane, the other being purely non-separable. The optimal limits exist, they are signal dependent and the found theoretical values are in accordance with the interference mid-point construction rule [4]. They may also be obtained by a simple geometric interpretation: the limit $\tau_{\max}(t,\omega)$ (resp. $\theta_{\max}(t,\omega)$) is the distance, measured parallel to the time-axis (resp. frequency-axis), between the autoterms causing the interference.

The product functions dispose of the separation capabilities for the autoterms and the interferences. More precisely, the time-product function allows the separation of time-interferences, while the frequency-product function mixes the components induced by autoterms and time-interferences and spreads them out on the whole space (t,ω,τ). Conversely, for frequency-interferences, the frequency-product function shows up separation capabilities.

These separation capabilities are a consequence of the particular geometry of the product functions which is illustrated in figure 1 for the time-product function. The same behaviour is valid for the frequency-product function. For a given time-frequency point, eventual autoterms are located close to the origin ($\tau \approx 0$) with positive amplitude. Interference terms, which complicate the interpretation of the TFD, are located at higher values of τ with positive or negative amplitudes. Components occuring at the same time but at a different frequency position may cause the superimposition of high-frequency oscillatory terms in the whole (t,ω,τ) space.

The optimal integration limits exclude the interference terms while preserving the auto terms.

3. ESTIMATION OF THE OPTIMAL INTEGRATION LIMITS

Given the interference geometry of the product functions presented in 2.2., the optimal integration limits consist of the maximum value τ which does not include the interference structures. To estimate these values $\tau_{\max}(t,\omega)$, we propose a two-step scheme, consisting of, firstly, the calculation of the smoothed-product functions and secondly, interference detection.

3.1. Smoothing of the Product Functions

In the time-product function, terms located at the same instant but at different frequencies cause the superimposition of highly oscillatory terms. To reduce the influence of these terms, we propose the smoothing of the time-product functions with a Gaussian separable bidimensional filter on the (t,τ) plane:

$$\bar{T}_{t,\omega}(\tau) = T_{t,\omega}(\tau) \underset{(\tau,t)}{\star} \left(\mathsf{G}_{\sigma_\tau}(\tau)\cdot \mathsf{G}_{\sigma_t}(t)\right)$$

where $\mathsf{G}_\sigma(\tau)$ is a Gaussian function with unity energy and variance σ. The filter-length parameters $\sigma_\tau(\tau)$ and $\sigma_t(\tau)$ are defined to be linearly decreasing with τ to account for the interference geometry. A similar filtering process is proposed for the frequency-product function on the (θ,ω) plane with filter lengths linearly decreasing with θ.

3.2. Detection of the Interference Terms

The second step of the estimation of the optimal integration limits consists in the detection of the terms indicating interferences in the smoothed-product functions (as shown by the solid lines of figure 1). The optimal time-limits are estimated as:

$$\tau_{\max}(t,\omega) = \min\left\{ \tau_0 \,\middle|\, \left(\bar{T}_{t,\omega}(\tau_0) - \min_{\tau_+<\tau<\tau_0} \bar{T}_{t,\omega}(\tau_0) > \lambda_+^T\right) \vee \left(\bar{T}_{t,\omega}(\tau_0) < \lambda_-^T\right) \right\}. \tag{5}$$

using an upper threshold λ_+ for positive valued interferences (case a and b in fig. 1) and a lower threshold λ_- for negative ones, defined as follows:

$$\lambda_+^T(\tau) = \lambda_0^T - \lambda_\Delta^T \cdot \tau, \qquad \lambda_-^T(\tau) = -\lambda_+^T(\tau). \tag{6}$$

As previously, the thresholds are chosen to be linearly decreasing with τ to account for the interference geometry. τ_+ is a small positive value chosen to avoid edge problems induced by the filtering.

This detection scheme is applied to the smoothed time-product function at each TF point to obtain $\tau_{\max}(t,\omega)$ and to the smoothed frequency-product function to obtain $\theta_{\max}(t,\omega)$.

4. THE LOCAL WIGNER-VILLE DISTRIBUTION

4.1. Definition

The optimal limits, estimated in the last section, give a detailed description of the interference geometry of the signal. We obtain the LWVD by the use of the separable filters of equation (2) but with the local filter-lengths $\tau_{\max}(t,\omega)$ and $\theta_{\max}(t,\omega)$ as estimated in section 3..

It should be pointed out that in evaluating the convolution integral of (3), the variables t, ω relative to $\tau_{\max}(t,\omega)$ and $\theta_{\max}(t,\omega)$ are kept constant. To handle this ambiguity, it is necessary to define two sets of time and frequency variables, one set in respect to the convolution with the filter (ω,t) and the other (t',ω') in respect to the dependency of the optimal limits on the actual TF point. The final distribution of equation (8) is obtained by setting both members of each set to the same values:

$$\mathsf{LWV}(t',\omega',t,\omega) = \Phi(t',\omega',t,\omega) \underset{(t,\omega)}{\star} \mathsf{WV}(t,\omega) \quad (7)$$

$$\mathsf{LWV}(t,\omega) = \mathsf{LWV}(t'=t,\omega'=\omega,t,\omega) \quad (8)$$

$$\Phi(t',\omega',t,\omega) = \\ = \frac{1}{2\pi} \underset{\substack{\tau\to\omega \\ \theta\to t}}{\mathcal{F}^{\,2\mathrm{D}}} \left\{ \mathrm{rect}_{\tau_{\max}(t',\omega')}(\tau) \cdot \mathrm{rect}_{\theta_{\max}(t',\omega')}(\theta) \right\}. \quad (9)$$

4.2. Properties

The LWVD may not be described by Cohen's class. However, recalling equation (7), it may be written as:

$$\mathsf{LWV}(t',\omega',t,\omega) = \underset{\substack{\tau\to\omega \\ \theta\to t}}{\mathcal{F}^{\,2\mathrm{D}}} \Big\{ \phi(t',\omega',\theta,\tau) \cdot A(\theta,\tau) \Big\}.$$

In this equation the ambiguity function $A(\theta,\tau)$ is weighted by a kernel $\phi(t',\omega',\theta,\tau)$ which depends explicitly on time t' and frequency ω'. In this sense, the class of LWVD may be seen as an extension of Cohen's class. The latter may be recovered using a time and frequency-independant kernel.

The class of LWVD may be characterised using this time-frequency dependent kernel $\phi(t',\omega',\theta,\tau)$. At the present time, we are able to give conditions to have the following properties satisfied:

- Shift-covariance[1]
$$\tilde{\phi}(t',\omega',\theta,\tau) = \phi(t'+t_0,\omega'+\omega_0,\theta,\tau)$$
- Scale-covariance
$$\tilde{\Phi}(t',\omega',t,\omega) = \Phi\left(at',\frac{\omega'}{a},at,\frac{\omega}{a}\right)$$
- Reality
$$\phi(t',\omega',\theta,\tau) = \phi(t',\omega',-\theta,-\tau)$$

The LWVD satisfies the shift-covariance and reality conditions while the scale-covariance condition is only satisfied for a particular class of signals. Only partial results have been obtained for the marginal distributions. It has been shown that time (resp. frequency) separable signals satisfy the time (resp. frequency) marginal. In these cases the energy is preserved.

5. EXAMPLES

5.1. An illustrative example

The signal considered is composed of two parallel chirps. Its WVD is shown on figure 2. As a particular example, we will present the different steps to reduce the interference term located at the origin ($t=0$, $\omega=0$). The first step consists in the computation of the time-product function represented for $\omega=0$ in figure 4. The interference term is centered around $t=0$, $\tau=32$ and the superimposed high-frequency oscillatory terms are well visible, while they are strongly removed in the smoothed time-product function (fig. 6). The detection of the interference term at $t=0$, $\omega=0$ is depicted on figure 5 and for this TF point the optimal limit is estimated as $\tau_{\max}(0,0)=8$.

This scheme is applied twice on each TF point to obtain all values of $\tau_{\max}(t,\omega)$ and $\theta_{\max}(t,\omega)$. The resulting LWVD of this example signal (fig. 3) shows the good interference reduction.

5.2. Signal "singauß'

The signal "singauß' is composed of two components, a chirp with a sinusoidal modulation law and a Gaussian centered at the origin. In the WVD of the signal (fig. 7), the Gaussian component is hidden by interferences. The LWVD (fig. 8) gives a better result than the optimal kernel method [1] (fig. 9). The interference reduction is much better and the autoterms are well conserved and not linearised and interrupted as in the case of the optimal kernel method.

6. CONCLUSIONS

We presented a TFD with locally adapted smoothing at each time-frequency point. The geometry of the interferences present in the WVD is described by optimal integration limits which are used to form an interference reduced TFD. This concept extends TFD only adaptive in time [2, 3] which are only capable of showing similar performances in the case of time-separable signals. A comparison of the results with those obtained by the optimal kernel method showed an increase of quality in the cases of synthetic and real vibration signals [5]. The LWVD may be described as an extension of Cohen's class by a kernel depending explicitly on time and frequency.

This work has to be continued in different ways. At the present time, we are developing a fast algorithm. Moreover, the replacement of the separable rectangular filter (eq. 9) by a separable Gaussian one may increase robustness, while non-separable filters may achieve even better results. Finally, the LWVD properties are still under study.

REFERENCES

[1] R. G. Baraniuk and D. L. Jones, "A signal-dependent time-frequency representation: optimal kernel design," *IEEE Transactions on Signal Processing*, vol. 41, no. 4, pp. 1589–1602, Apr. 1993.

[2] R. N. Czerwinski and D. L. Jones, "Adaptive cone-kernel time-frequency analysis," *IEEE Transactions on Signal Processing*, vol. 43, no. 7, pp. 1715–1719, July 1995.

[3] D. L. Jones and R. G. Baraniuk, "An adaptive optimal-kernel time-frequency representation," *IEEE Transactions on Signal Processing*, vol. 43, no. 10, pp. 2361–2371, Oct. 1995.

[4] P. Flandrin, *Temps-fréquence*, Hermés, Paris, 1993.

[5] H. Oehlmann, *Analyse temps-fréquence de signaux vibratoires de boîtes de vitesses*, Ph.D. thesis, Doctorat de l'Université Henri Poincaré, Nancy I, 15 July 1996.

[1] The kernel $\tilde{\phi}$ corresponds to the shifted or scaled signals.

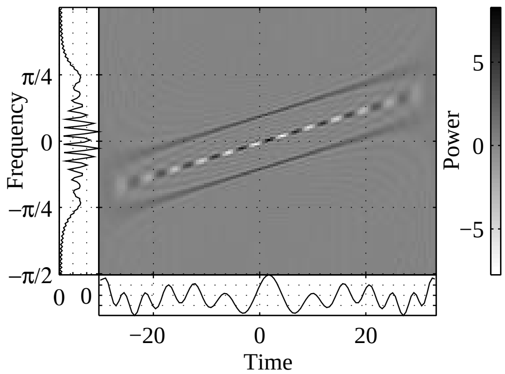

Figure 2. WVD of the signal “road”

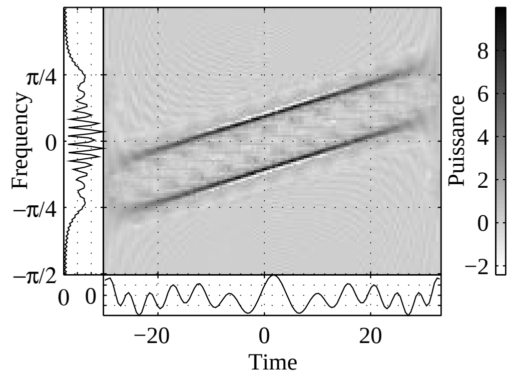

Figure 3. LWVD of the signal ”road”

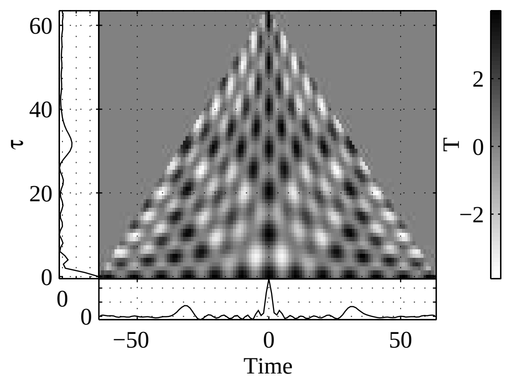

Figure 4. Time-Product function $T_{t,0}(\tau)$ for $\omega = 0$

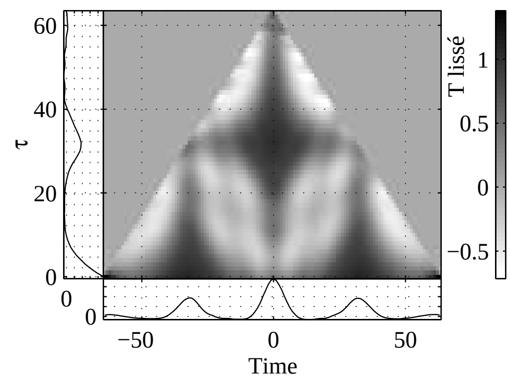

Figure 5. Smoothed time-product function $\bar{T}_{t,0}(\tau)$ for $\omega = 0$

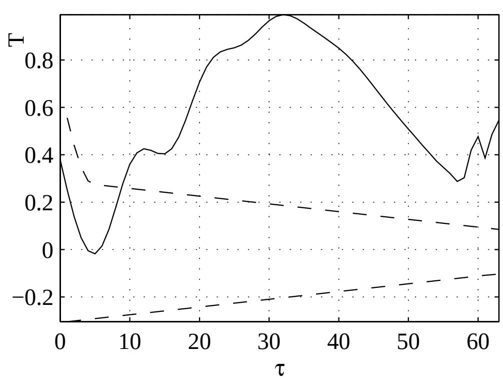

Figure 6. Estimation at $t = 0$, $\omega = 0$: $\bar{T}_{0,0}(\tau)$ (solid), thresholds (dashed)

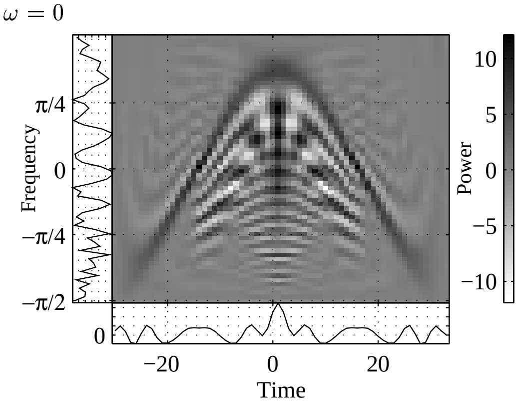

Figure 7. WVD of the signal “singauß”

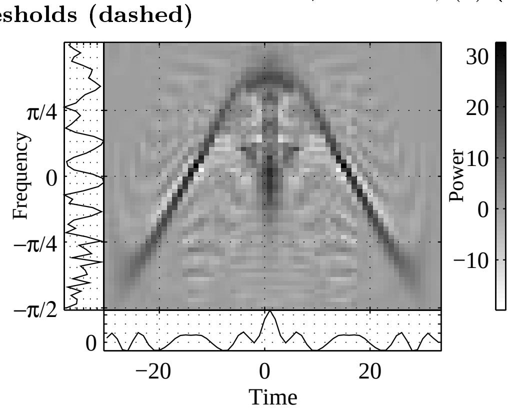

Figure 8. LWVD of the signal ”singauß”

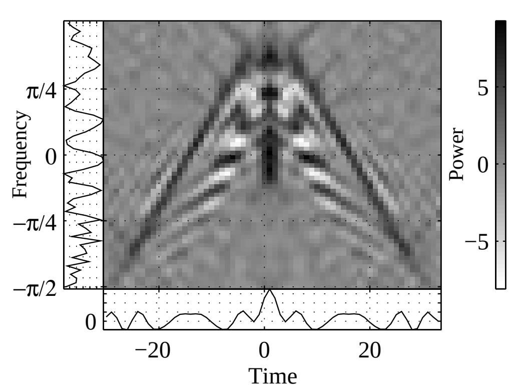

Figure 9. Optimal kernel distribution of ”singauß”